Atmos. Chem. Phys. Discuss., 11, 13867–13910, 2011
www.atmos-chem-phys-discuss.net/11/13867/2011/
doi:10.5194/acpd-11-13867-2011

Atmospheric Chemistry and Physics Discussions

Springtime carbon episodes at Gosan background site revealed by total carbon, stable carbon isotopic composition, and thermal characteristics of carbonaceous particles

J. Jung and K. Kawamura

Institute of Low Temperature Science, Hokkaido University, Sapporo 060-0819, Japan

Received: 30 March 2011 – Accepted: 27 April 2011 – Published: 6 May 2011

Correspondence to: K. Kawamura (kawamura@lowtem.hokudai.ac.jp)

Published by Copernicus Publications on behalf of the European Geosciences Union.

Abstract

In order to investigate the carbon episodes at Gosan background super-site (33.17° N, 126.10° E) in East Asia during spring of 2007 and 2008, total suspended particles (TSP) were collected and analyzed for particulate organic carbon, elemental carbon, total carbon (TC), total nitrogen (TN), and stable carbon isotopic composition ($\delta^{13}C$) of TC. The carbon episodes at the Gosan site were categorized as long-range transported anthropogenic pollutant (LTP) from Asian continent, Asian dust (AD) accompanying with LTP, and local pollen episodes. The stable carbon isotopic composition of TC ($\delta^{13}C_{TC}$) was found to be lowest during the pollen episodes (range: −26.2‰ to −23.5‰, avg.: −25.2 ± 0.9‰), followed by the LTP episodes (range: −23.5‰ to −23.0‰, avg.: −23.3 ± 0.3‰) and the AD episodes (range: −23.3 to −20.4‰, avg.: −21.8 ± 2.0‰). The $\delta^{13}C_{TC}$ of the airborne pollens (−28.0‰) collected at the Gosan site showed value similar to that of tangerine fruit (−28.1‰) produced from Jeju Island. Based on the carbon isotope mass balance equation and the TN and TC regression approach, we found that ~ 40–45 % of TC in the TSP samples during the pollen episodes was attributed to airborne pollens from Japanese cedar trees planted around tangerine farms in Jeju Island. The $\delta^{13}C$ of citric acid in the airborne pollens (−26.3‰) collected at the Gosan site was similar to that in tangerine fruit (−27.4‰). The negative correlation between the citric acid-carbon/TC ratios and $\delta^{13}C_{TC}$ were obtained during the pollen episodes. These results suggest that citric acid emitted from tangerine fruit may be adsorbed on the airborne pollens and then transported to the Gosan site. Based on the thermal evolution pattern of organic aerosols during the carbon episodes, we found that organic aerosols originated from East China are more volatile on heating and are more likely to form pyrolized organic carbon than the pollen-enriched organic aerosols and organic aerosols originated from Northeast China. Since thermal evolution patterns of organic aerosols are highly influenced by their molecular weight, they can be used as additional information on the formation of secondary organic aerosols during the long-range atmospheric transport and the source regions of organics.

ACPD
11, 13867–13910, 2011

1 Introduction

Carbonaceous aerosols that comprise elemental carbon (EC) and organic carbon (OC) have large impacts on human health (Baltensperger et al., 2008), visibility impairment (IMPROVE, 2006), and radiation budget in the atmosphere (IPCC, 2007). Organic aerosols are primarily emitted from various sources and secondarily produced in the atmosphere by oxidation of volatile organic compounds followed by condensation on pre-existing particles and/or nucleation. In regions affected by anthropogenic pollutants, organic aerosols may play an important role in determining the climate effect of clouds as sulfate aerosols (Novakov and Penner, 1993). Model simulation results indicate that organic aerosol can enhance the cloud droplet concentration and is therefore an important component of the aerosol-cloud-climate feedback system (O'Dowd et al., 2004).

Jeju Island, Korea, is located at the boundary of the Yellow Sea and the East China Sea and is surrounded by mainland China, Korean Peninsular, and Kyushu Island, Japan. Gosan site is located on the western edge of Jeju Island facing the Asian continent and is isolated from residential areas of the island (Kawamura et al., 2004). In order to understand physicochemical and radiative properties of anthropogenic aerosols under Asian continental outflow, several international experiments have been conducted at the Gosan site such as ACE-Asia (Aerosol Characterization Experiment-Asia) (Huebert et al., 2003) and ABC-EAREX 2005 (Atmospheric Brown Cloud-East Asia Regional Experiment 2005) (Nakajima et al., 2007). To better understand the link between chemical and physical properties of aerosols mainly transported from Asian continent and regional climate change, sources and formation mechanism of secondary aerosols should be investigated. In addition, contributions of local effects on the Gosan site aerosols should be qualitatively and quantitatively evaluated.

Pollen is one of the important sources of bioaerosols (Solomon, 2002). They can cause serious allergic problems to human health (Solomon, 2002) and visibility impairment (Kim, 2007). Most pollen blowing events occur during the growing season

ACPD
11, 13867–13910, 2011

of plants from March to May in Korea (Oh et al., 1998). Since airborne pollen can be transported very long distance (Porsbjerg et al., 2003; Rousseau et al., 2008), airborne pollen is not only local problem but also regional and intercontinental problems. Airborne pollens from local plants in Jeju Island can cause an increase in organic aerosol mass and may overestimate relevant radiative forcing by in situ observations compared to a prediction by chemical transport model (Huebert et al., 2003). However, there were rare studies regarding the impact of the pollens on the aerosol chemical composition at the Gosan site (Jung and Kawamura, 2011).

Stable carbon isotopic compositions ($\delta^{13}C$) of total carbon (TC) are very useful for investigating sources and long-range atmospheric transport of organic aerosols (Cachier et al., 1986; Narukawa et al., 2008; Miyazaki et al., 2010). On the basis of the $\delta^{13}C$ values and Na^{+}/TC ratios, Narukawa et al. (2008) estimated the contribution of marine organic matter in TC in the high Arctic at Alert during spring. Miyazaki et al. (2010) estimated marine-derived carbon in TC over the western North Pacific using $\delta^{13}C$ values. Recently, Kawamura and Watanabe (2004) developed a novel method for compound specific carbon isotope compositions of dicarboxylic acids and related compounds using a gas chromatography/isotope ratio mass spectrometry (GC/irMS). Since then, $\delta^{13}C$ values of dicarboxylic acids and related compounds has successfully been used to assess the extent of photochemical processing of aerosols during the long-range atmospheric transport (Wang and Kawamura, 2006; Aggarwal and Kawamura, 2008).

In this study, elevated concentrations of carbon were often obtained in the total suspended particulate (TSP) samples collected at the Gosan site in spring of 2007 and 2008. Using remote monitoring and comprehensive in-situ chemical and $\delta^{13}C$ analyses, we categorize the carbon episodes to three groups; long-range transport anthropogenic pollution (LTP) from Asian continent, Asian dust (AD) accompanying with the LTP, and local airborne pollen episodes. We discuss the $\delta^{13}C$ measured and the thermal evolution pattern obtained upon heating of carbonaceous particles in terms of their source regions. Based on the carbon isotope mass balance equation and the TN and

ACPD
11, 13867–13910, 2011

TC regression approach, we quantify the fraction of local pollens in TC measurement. Using the HCl fume treatment on the dust-enriched sample, we quantify carbonate carbon in TC and discuss removal of carbonate via the reaction with acidic gases during the long-range atmospheric transport.

2 Samples and methods

TSP sampling was carried out at the Gosan supersite (33.17° N, 126.10° E) in PlaceNameJeju Island, located approximately 100 km south of the Korean Peninsula, over 2–5 days integration during 23 March to 1 June of 2007 and 16–24 April of 2008. TSP samples were collected on pre-combusted quartz fiber filters (20 × 25 cm) using a high volume air sampler (Kimoto AS-810) installed on the rooftop of a trailer (~ 3 m above the ground). Before and after sampling, the filter samples were stored in clean glass jars (150 ml) with a Teflon-lined screw cap at −20 °C prior to analysis. Field blank filters were collected every month. Hourly PM_{10} mass data was obtained from the National Institute of Environment Research at the Gosan observatory. Total 32 filter samples were analyzed in this study.

2.1 Airborne pollen and tangerine fruit samples

Three types of pollen samples were prepared and analyzed in this study. Two authentic standard pollen samples from Japanese cedar (Pollen_cedar) and Japanese cypress (Pollen_cypress) were obtained from the WAKO Chemical Co. (product No. 168-20911 for Japanese cedar and 165-20921 for Japanese cypress). Additionally, airborne pollens (Pollen_Gosan), which were mainly originated from Japanese cedar trees planted around tangerine farms in Jeju Island, were separated from an aliquot of the TSP filter sample collected during the severe pollen episode period (KOS751, 16–21 April 2008) using mild vibration. Tangerine fruit produced from Jeju Island was also prepared. In order to prevent possible contamination over the surface of tangerine fruit, tangerine surface was mildly washed using ultra pure organic-free Milli-Q water three times.

ACPD
11, 13867–13910, 2011

2.2 Organic and elemental carbon analysis

Organic carbon (OC) and elemental carbon (EC) were analyzed by a Sunset carbon analyzer using the thermal-optical transmittance (TOT) protocol for pyrolysis correction (Birch and Cary, 1996; Miyazaki et al., 2009). A 2.14 cm^2 punch of the quartz filter was placed in a quartz boat inside the thermal desorption chamber of the analyzer. The OC and EC were determined under a prescribed temperature protocol in an inert atmosphere (100 % He) and in an oxidizing atmosphere (He/10 % O_2 mixture), respectively. The OC detected in temperature steps of 300 °C, 450 °C, 600 °C, and 650 °C are defined as OC1, OC2, OC3, and OC4, respectively. The EC detected in temperature steps of 550 °C, 625 °C, 700 °C, 775 °C, 850 °C, and 870 °C are defined as EC1, EC2, EC3, EC4, EC5, and EC6, respectively. The pyrolized organic carbon (PC), which was converted from OC in the inert mode of the analysis, was corrected by monitoring the transmittance of a pulsed He-Ne diode laser beam through the quartz fiber filter. External calibration was performed before the analysis using a known amount of sucrose. The detection limits of OC and EC, which are defined as three times of standard deviation of field blanks, were 0.26 and 0.01 $\mu g\,C\,m^{-3}$. However, these values are quite small compared to the instrument's minimum quantifiable level of 0.5 $\mu g\,C\,m^{-3}$ given by the manufacturer. Therefore, 0.5 $\mu g\,C\,m^{-3}$ was considered as the detection limit of both OC and EC. The analytical errors, which are defined as the ratio of the standard deviation to the average value obtained from the triplicate analyses of the filter sample, of OC and EC measurements were 5 % and 3 %, respectively.

2.3 Determination of water-soluble inorganic ions

To measure water-soluble inorganic ions, an aliquot (2.01 cm^2) of the quartz filter was extracted with 10 ml of the Milli-Q water under ultrasonication (30 min) and then passed through a disk filter (Millipore, Millex-GV, 0.45 µm). The concentrations of cations in the water extracts were measured using an ion chromatography (Metrohm, 761). The sodium (Na^+) and calcium (Ca^{2+}) were determined using an Metrosep C2 column

ACPD
11, 13867–13910, 2011

(150 mm) with 4 mM tartaric acid/1 mM 2,6-pyridinedicarboxylic acid as an eluent (flow rate: 1.0 ml min^{-1}, sample loop volume: 200 µl, time eluted: 30 min). The analytical error of Ca^{2+} based on the triplicate analyses of filter sample was 1.1 %. The Ca^{2+} concentration was corrected for sea-salt fraction using Na^{+} as a sea-salt tracer and used in this study. It is found that ~92 % of Ca^{2+} was attributed to non-sea-salt Ca^{2+} (nss-Ca^{2+}). All the concentrations of OC, EC, and nss-Ca^{2+} reported here are corrected for field blanks.

2.4 Total carbon, total nitrogen, and carbon isotope analysis

Total carbon (TC) and total nitrogen (TN) were measured by an elemental analyzer (EA) (Carlo Erba, NA 1500) whereas stable carbon isotope ($\delta^{13}C$) analyses were conducted using the same EA interfaced to an isotope ratio mass spectrometer (irMS) (Finnigan MAT Delta Plus) (Kawamura et al., 2004). An aliquot of filter sample (2.01 cm^2) was placed in a tin cup, introduced into the EA and then were oxidized in a combustion column packed with chromium(III) oxide at 1020 °C. Nitrogen oxides coming from the combustion column were reduced to molecular nitrogen (N_2) in a reduction column packed with metallic copper at 650 °C. The derived N_2 and carbon dioxide (CO_2) were isolated using a gas chromatograph (GC) installed in the EA and then measured with a thermal conductivity detector. An aliquot of CO_2 gases was then introduced to the irMS through an interface (ThermoQuest, ConFlo II). The stable carbon isotopic composition ($\delta^{13}C$) relative to the Pee Dee Belemnite (PDB) standard was calculated using the standard isotopic conversion equation as follows.

$$\delta^{13}C\,(‰) = \left[\frac{(^{13}C/^{12}C)_{sample}}{(^{13}C/^{12}C)_{standard}} - 1\right] \times 1000$$

External calibration was conducted using known amounts of acetanilide in order to calculate mass concentrations of TC and TN and $\delta^{13}C$ of TC ($\delta^{13}C_{TC}$). The mass concentrations and $\delta^{13}C_{TC}$ values reported here were corrected against the field blanks

ACPD
11, 13867–13910, 2011

using isotope mass balance equations (Turekian et al., 2003). The blank levels of TC and TN mass concentrations were 2.0 % and 1.3 % of the measured concentrations, respectively. The analytical errors for TC and TN mass concentrations based on the triplicate analyses of the filter sample were 2.3 % and 5.2 %, respectively. The standard deviation of $\delta^{13}C_{TC}$ based on the triplicate analyses of the filter sample were 0.03 ‰ and its analytical error was 0.1 %. In order to remove carbonate carbon from the dust-enriched filter samples, aliquots of the samples were treated with HCl fume as the method described by Kawamura et al. (2004) and Kundu et al. (2010). Each filter cut of the dust-enriched samples was placed in a 50 ml glass vial and exposed to the HCl fume overnight in a glass desiccator (10 l). The HCl treated filter samples were then analyzed for TC mass and $\delta^{13}C_{TC}$ as described above.

The $\delta^{13}C$ values of the water-soluble fraction of the filter samples were also analyzed in this study as follows. Aliquots of the TSP filter and pollen samples were extracted with the Milli–Q water under ultrasonication (5 min × 3 times) and then passed through a disk filter (Millipore, Millex–GV, 0.45 µm) to remove water-insoluble suspended particles and filter debris. After concentrating the filtered water extracts using a rotary evaporator, the samples were applied by a micro glass syringe to the prebaked quartz filters and then dried using silica gel overnight in a glass desiccator. Finally, the prepared samples were analyzed for $\delta^{13}C_{TC}$ using the same technique used for the bulk filter sample analysis.

2.5 Stable carbon isotopic compositions of the major dicarboxylic acids and related compounds

The $\delta^{13}C$ values of the major dicarboxylic acids and citric acid were measured using the method developed by Kawamura and Watanabe (2004). Diacids and citric acid in the TSP samples were reacted with 14 % BF_3 in 1-butanol at 100 °C for 60 min to derive butyl esters (Kawamura, 1993; Jung and Kawamura, 2011). After an appropriate amount of internal standard (*n*-alkane C_{13}) was spiked to an aliquot of the derivatives,

ACPD
11, 13867–13910, 2011

δ^{13}C values of the esters were measured using a GC (Hewlett-Packard, HP6890) interfaced to the irMS. The δ^{13}C values of free organic acids were then calculated by the isotopic mass balance equation using the measured δ^{13}C of the derivatives and the derivatizing agent (1-butanol) (Kawamura and Watanabe, 2004). Each sample was analyzed in duplicates, and the average δ^{13}C values of the quantified compounds were reported. Prior to actual sample analysis, we confirmed that the δ^{13}C values of the working standards (a mixture of normal C_{15}–C_{34} alkanes) were equivalent to the theoretical values within an analytical error of 0.2‰. In this paper we report δ^{13}C values for oxalic and citric acids.

3 Classification of atmospheric conditions

Air mass backward trajectories and satellite aerosol optical thickness (AOT) can be utilized to characterize potential source regions and transport pathway of air masses. Air mass backward trajectories that ended at the measurement site were computed for 500 m height above ground level using the HYSPLIT (HYbrid Single-Particle Lagrangian Trajectory) backward trajectory analysis (Draxler and Rolph, 2011; Rolph, 2011). All calculated backward trajectories extended 96 h backward with a 1-h interval. AOT values retrieved by the new version V5.2 of the NASA MODIS (Moderate Resolution Imaging Spectro-radiometer) algorithm, called Collection 005 (C005) (Levy et al., 2007a,b), were used in this study. AOT data which are part of the MODIS Terra/Aqua Level-2 gridded atmospheric data product are available on the MODIS web site (http://modis.gsfc.nasa.gov/). Remer et al. (2005) reported the associated errors of MODIS AOT with $\pm(0.05+0.15\cdot\mathrm{AOT})$ and $\pm(0.03+0.05\cdot\mathrm{AOT})$ over land and ocean, respectively.

Aerosol Ångström exponent (α) calculated from the AOT values at 440 and 870 nm measured by a sunphotometer were obtained from the Gosan AERONET site (http://aeronet.gsfc.nasa.gov). In order to estimate α values during the cloudy days of the sampling periods at the Gosan site, α values were also obtained from the Gwangju AERONET site (126°50′ E, 35°13′ N), which is located at ~200 km north of the Gosan

ACPD
11, 13867–13910, 2011

site. During the episodic periods, excellent agreement of the α values was observed between the two sites with the regression slope of 1.04 ($R^2 = 0.95$). Thus, we alternatively used α values obtained from the Gwangju AERONET site for the cloudy days of the sampling periods (KOS606, 608, and 751) at the Gosan site (Table 1). Cloud-screened and quality-assured Level 2.0 sunphotometer data determined by the AERONET algorithm (Dubovik and King, 2000) were used in this study.

Temporal variations of mass concentrations of PM_{10}, TC, and TN, $\delta^{13}C_{TC}$, and TC/TN mass ratios during the entire sampling periods are shown in Fig. 2. Three carbon episodes such as long-range transported pollutants (LTP), Asian dust (AD) accompanying with LTP, and local pollen episodes were observed as marked in Fig. 2 and summarized in Table 1. This study defined the carbon episode as average mass concentration of TC > 10 $\mu g\,C\,m^{-3}$. The MODIS AOT and α values during the selected day (7 April 2007) of the LTP episodes showed that severe haze lingered over eastern part of China, extending over the Yellow Sea and our measurement site (Fig. 3a,b). The α represents the wavelength (λ) dependence of AOT ($= -d\log AOT/d\log\lambda$). A small α indicates the presence of particles with a large size, and vice versa. Thus, a high AOT > 1.0 and high $\alpha > 1.0$ on 7 April 2007 indicated the presence of anthropogenic haze aerosols. Air mass backward trajectories during the LTP episodes showed two major air mass transport patterns; one from East China (LTP_EC) and the other from Northeast China (LTP_NEC) (Fig. 4). Air masses during the LTP_EC episodes (KOS606, 614, and 619) were mainly originated from the areas between Beijing and Shanghai, implying that pollution aerosols emitted from East China had an impact on the measurement site. However, air masses during the LTP_NEC episodes (KOS621 and KOS623) were mainly originated from the areas between Beijing and northern part of China. Similar levels of PM_{10} mass concentrations were obtained during the LTP_EC and LTP_NEC episodes with an average of 70 to 129 $\mu g\,m^{-3}$ and 74 to 107 $\mu g\,m^{-3}$, respectively. However, the α calculated from the AERONET AOT showed lower values during the LTP_NEC episodes (avg. 0.65 to 0.86) than those during the LTP_EC episodes (avg. 1.28 to 1.40), indicating larger particle sizes during the LTP_NEC episodes.

ACPD
11, 13867–13910, 2011

Two AD episodes were observed during 30 March–2 April 2007 (KOS603) and 25–28 May 2007 (KOS627). A high AOT > 1.0 and low $\alpha < 0.4$ during the selected day (31 March 2007) of the AD episodes clearly showed the presence of dust plumes over the Yellow Sea (Fig. 3c,d). The α obtained from the AERONET AOT also showed low values (0.37 ± 0.06) during the KOS627 AD episode (Table 1), indicating large size particles in the dust plumes. The elevated concentrations of nss-Ca^{2+} (>7.0 µg m^{-3}) in the KOS603 and KOS627 filter samples supported the presence of dust particles (Table 1). Air mass backward trajectories during the AD episodes clearly showed that dust particles mainly originated from the Nei Mongol desert in China transported to the measurement site across the Yellow Sea (Fig. 4). During the AD episodes, average PM_{10} mass concentrations were obtained to be 362 and 157 µg m^{-3} with peak values of 3704 and 286 µg m^{-3} for the KOS603 and KOS627 sampling periods, respectively.

Pollen episodes, which were mainly caused by pollens from Japanese cedar trees planted around tangerine farms, were observed at the Gosan site during mid- to late April of 2007 and 2008 (Jung and Kawamura, 2011). Jung and Kawamura (2011) reported the enhanced concentration of citric acid, which may be directly emitted from tangerine fruit during the pollen episodes, likely adsorbed on pollens from Japanese cedar trees and then transported to the Gosan site. Identification of pollen episodes was conducted based on daily human observation of pollen blowing and the microscopic image of pollens collected in the TSP samples. Total 8 pollen-enriched TSP samples were collected during 11–23 April of 2007 and 16–24 April of 2008 (Table 1).

4 Results and discussion

4.1 TC and TN mass concentrations during the carbon episodes

Similar TC mass concentrations were obtained during the three carbon episodes ranging avg. 15 ± 6.0 µg C m^{-3} to avg. 16 ± 6.7 µg C m^{-3} (Table 2). Similar amounts of OC and EC as well as TC during the LTP (LPT_EC plus LTP_NEC) and AD episodes as

ACPD
11, 13867–13910, 2011

shown in Table 2 indicated that the AD episodes in spring are frequently accompanied with anthropogenic pollutants emitted from the industrial regions of East China and Northeast China. However, relatively high mass concentrations of TN (avg. 11 ± 8.2 $\mu g\,N\,m^{-3}$) were obtained during the LTP episodes, followed by the AD episodes (avg. 7.7 ± 4.0 $\mu g\,N\,m^{-3}$) and the Pollen episodes (avg. 4.8 ± 1.5 $\mu g\,N\,m^{-3}$). Much higher TC/TN mass concentration ratios (avg.: 3.5 ± 1.2, range: 1.8 to 5.3) were observed during the pollen episodes than those during the LTP episodes (avg.: 1.6 ± 0.58, range: 0.96 to 2.3) mainly due to the enhanced organic carbon mass by airborne pollens. The highest OC/EC ratios (avg.: 5.8 ± 2.6, range: 3.8 to 12) were also obtained during the pollen episodes, supporting the enhanced organic carbon mass by airborne pollens.

Excellent correlation ($R^2 = 0.95$) was obtained between mass concentrations of TN and TC during the LTP periods (Fig. 5a), implying similar sources of TN and TC. A strong correlation between mass concentrations of TN and TC was also obtained during the LTP plus non-episodic periods ($R^2 = 0.82$) (Fig. 5b), suggesting that aerosols during the non-episodic periods in spring might be influenced by the LTP aerosols from the Asian continent. However, poor correlations of TN vs. TC mass concentrations were obtained during the pollen episodes (Fig. 5a). Even though similar levels of TN were obtained during the pollen episodes, TC values were highly variable ranging 7.5 to 28 $\mu g\,C\,m^{-3}$ mainly due to the different strength of pollen blowing and meteorological conditions (Doskey and Ugoagwu, 1989; Puc and Wolski, 2002; Palacios et al., 2007).

TC and TN mass concentrations obtained during the LTP plus non-episodic periods are compared to those from previous studies in the Asian continent (Fig. 5b). TC and TN concentrations in the Asian continent were obtained from the Hua mountain site (PM_{10}, winter) in China (Li et al., 2011) and the urban cities of China; Shanghai ($PM_{2.5}$, winter and spring) (Ye et al., 2003), Nanjing ($PM_{2.5}$, winter) (Yang et al., 2005), Baoji (PM_{10}, spring) (Wang et al., 2010). TN values in the Asian continent were calculated from nitrogen mass in particulate nitrate and ammonium. Kundu et al. (2010) reported that ~97 % of TN at the Gosan site was explained by nitrate and ammonium nitrogen. Thus, the contribution of organic nitrogen to TN is negligible at the Gosan

ACPD
11, 13867–13910, 2011

site. Excellent correlation ($R^2 = 0.98$) was obtained between TC and TN mass concentrations in the Asian continent (Fig. 5b). Interestingly, the slope (2.83) of TN versus TC mass concentrations (avg. TC/TN mass ratio = 3.2 ± 0.63) in the Asian continent was much higher than that (0.83) for the LTP plus non-episode samples (avg. TC/TN mass ratio = 1.7 ± 0.57) at the Gosan site. About twice lower TC/TN mass ratios at the Gosan site suggested that the formation mechanisms of aerosol phase nitrogen and secondary organic aerosols are quite different during the long-range atmospheric transport. Different dry and wet deposition rates between nitrogen containing particles and organic aerosols may also be attributed to these differences.

Using the regression slope of TN versus TC mass concentrations during the LTP plus non-episodic periods that may represent normal atmospheric condition at the Gosan site in spring, the contribution of the airborne pollen carbon in TC can be roughly calculated as follows;

$$\text{TC\_pollen}\,(\mu\text{g C m}^{-3}) = \text{TC}\,(\mu\text{g C m}^{-3}) - (0.83 \cdot \text{TN}\,(\mu\text{g N m}^{-3}) + 3.79) \quad (1)$$

The contribution of the airborne pollen carbon to TC was roughly estimated to be 20 % to 71 % with an average of 46 ± 19 %.

TC/TN mass concentration ratio (3.9) in the strong AD episode sample (KOS603) was much higher than that (1.2) in the weaker AD episode sample (KOS627) (Fig. 5a). The enhanced mass concentration of TC in the KOS603 sample may be in part attributed to the presence of carbonate carbon in dust particle, which was not removed completely via the reaction with nitrogen dioxide (NO_2), nitric acid (HNO_3), and sulfur dioxide (SO_2) (Zhang et al., 1994; Mamane and Gottlieb, 1989; Underwood et al., 2001) during the long-range atmospheric transport. The enhanced carbonate carbon in TC during the strong AD episode will be discussed in detail in Sect. 4.2.

ACPD
11, 13867–13910, 2011

4.2 Stable carbon isotopic composition of TC during the carbon episodes

The $\delta^{13}C$ values of TC ($\delta^{13}C_{TC}$) during the carbon episodes are plotted as a function of TC mass concentrations in Fig. 6a and summarized in Table 2. The $\delta^{13}C_{TC}$ values during the LTP episodes ranged from −23.5 ‰ to −23.0 ‰ with an average of −23.3 ± 0.3 ‰. Similar $\delta^{13}C_{TC}$ values were observed regardless of TC mass concentrations during the LTP episodes (Fig. 6a). However, the $\delta^{13}C_{TC}$ during the pollen episodes showed more negative values ranging −26.2 ‰ to −23.5 ‰ with an average of −25.2 ± 0.9 ‰. The $\delta^{13}C_{TC}$ values for the AD episodes are relatively high ranging −23.3 ‰ to −20.4 ‰ with an average of −21.8 ± 2.0 ‰. These results suggested that $\delta^{13}C_{TC}$ can be utilized as an indicator of the possible sources of the carbon episodes at the Gosan site with the relatively low values during the pollen episodes than those during the LTP and AD episodes.

The $\delta^{13}C_{TC}$ during the strong AD episode (KOS603) gave higher value than the weaker AD episode (KOS627) as shown in Fig. 6a. In order to quantify the effect of carbonate in dust particle on the TC mass and $\delta^{13}C_{TC}$ measurements, the HCl fume treated filter samples during the AD episodes were also analyzed for TC mass and $\delta^{13}C_{TC}$. It was clearly observed that the TC mass concentration and $\delta^{13}C_{TC}$ in the KOS603 sample decreased from 18.8 μg C m^{-3} to 14.7 μg C m^{-3} and from −20.4 ‰ to −22.1 ‰ by the HCl fume treatment. However, those in the KOS627 sample were invariant before and after the HCl treatment (Fig. 6b). The removed carbon (removed_C) that was calculated from the difference between TC mass concentrations before and after the HCl fume treatment was obtained to be 4.1 μg C m^{-3} for the KOS603 sample.

In order to characterize the carbonate carbon in the removed_C, the $\delta^{13}C$ of the removed_C ($\delta^{13}C_{removed\_C}$) was calculated using the isotopic mass balance equation as follows (Kawamura et al., 2004);

$$\delta^{13}C_{TC} = \frac{remained\_C}{TC} \cdot \delta^{13}C_{remained\_C} + \frac{removed\_C}{TC} \cdot \delta^{13}C_{removed\_C} \quad (2)$$

ACPD
11, 13867–13910, 2011

The $\delta^{13}C_{removed\_C}$ in the KOS603 sample was calculated as −14.1 ‰. This value was higher than that of the remained_C while much lower than those (−1.3 to −0.3 ‰) of the standard Asian dust samples collected from the Gunsu Province, China (Kawamura et al., 2004), indicating that not only carbonate carbon but also volatile organic acids adsorbed on aerosol particles were removed by the HCl fume treatment. Kawamura et al. (2004) suggested that low molecular weight organic acids such as formic, acetic, and oxalic acids are possible candidates for the removed volatile and semi-volatile organic acids. By assuming that the $\delta^{13}C$ of the removed organic acids has the same $\delta^{13}C$ of the remained_C, carbonate carbon in the KOS603 sample was roughly estimated as 1.5 μg C m^{-3} (8 % in TC) using the isotopic mass balance Eq. (2) and the $\delta^{13}C$ of the removed carbonate of −0.3 ‰ by Kawamura et al. (2004).

Calcium carbonate in dust particle reacts with nitrogen dioxide (NO_2), nitric acid (HNO_3), and sulfur dioxide (SO_2) to produce calcium nitrate and calcium sulfate (Zhang et al., 1994; Mamane and Gottlieb, 1989; Underwood et al., 2001). The presence of carbonate in the KOS603 sample indicated insufficient amounts of gas phase NO_2, HNO_3, and SO_2 to remove all carbonate during the long-range atmospheric transport. Much higher TC/TN ratio during the strong AD episode (KOS603) was also attributed to the remained carbonate carbon. However, negligible amount of carbonate in the KOS627 sample indicated that most carbonate was removed via the reaction with NO_2, HNO_3, and SO_2 during the long-range atmospheric transport. Relatively high TN mass in the KOS627 sample also supported the efficient removal of carbonate via the reaction with HNO_3.

4.3 Impact of airborne pollens on TC measurement

4.3.1 The $\delta^{13}C$ of TC in airborne pollens and tangerine fruit

The $\delta^{13}C_{TC}$ in airborne pollens and tangerine fruit are shown in Fig. 7 and Table 3. The $\delta^{13}C$ of the water-soluble fractions of the pollens are also shown in Fig. 7. Much lower $\delta^{13}C_{TC}$ value was obtained in the Pollen_Gosan (−28.0 ‰) than the authentic

ACPD
11, 13867–13910, 2011

standard pollens; −25.4‰ for the Pollen_cedar and −23.3‰ for the Pollen_cypress. The $\delta^{13}C_{\_TC}$ in the Pollen_Gosan was slightly lower than the average value (−26.8‰) of 174 different species of pollen samples from C_3 plants across the US (Jahren, 2004). This difference may be attributed to the geographical difference of the pollen samples. Jahren (2004) reported the the $\delta^{13}C_{TC}$ values (−30.2‰ to −24.5‰) in the pollens from C_3 plants depend on geographical locations and types of C_3 plants. Interestingly, the $\delta^{13}C_{TC}$ in the tangerine peel (−28.1‰) was very similar to that in the Pollen_Gosan. Slightly higher $\delta^{13}C_{TC}$ (−27.0‰) was obtained in the tangerine juice than tangerine peel.

The $\delta^{13}C$ values of the water-soluble fraction of the pollens were obtained to be −24.7‰, −26.1‰, and −25.0‰ for the Pollen_Gosan, Pollen_cedar, and Pollen_cypress, respectively. The value for the Pollen_Gosan was slightly higher than that of the bulk Pollen_Gosan. However, the $\delta^{13}C$ of the water-soluble fraction in the Pollen_cedar and Pollen_cypress were slightly lower than the bulk pollens (Table 3). These results imply that the water-soluble fraction of the Pollen_cedar and Pollen_cypress might be originated from different sources and be adsorbed to the pollens.

In order to estimate the contribution of the airborne pollen carbon to aerosol TC during the pollen episodes, the carbon mass derived from the airborne pollens were determined using the isotopic mass balance equation in Eq. (2). Since most of aerosols at the Gosan site in spring were influenced by the long-range transport of anthropogenic aerosols from the Asian continent as discussed in Sect. 4.1, we assumed that carbonaceous particles during the pollen episodes were mainly originated from the airborne pollens and the long-range transported organic pollutants. Thus, the $\delta^{13}C_{\_TC}$ in the Pollen_Gosan (−28.0‰) and average $\delta^{13}C_{\_TC}$ during the LTP episodes (−23.3‰) were used as two end members to calculate the airborne pollen carbon mass (TC_pollen). The TC_pollen concentrations were determined to be 0.4 to 16.7 μg C m^{-3} (4 to 62 % in TC) with a median of 5.1 μg C m^{-3} (42 %) during the pollen episodes (Fig. 8). The median value of the TC_pollen fraction in TC was quite similar to

ACPD
11, 13867–13910, 2011

that obtained using the TN and TC regression approach in Eq. (1). Thus, it was found that ~40–45 % of TC in the TSP samples at the Gosan site were attributed to the airborne pollens during the pollen episodes. These local pollens can cause an enhanced organic aerosol mass and may overestimate the relevant radiative forcing at the Gosan site. These results can provide useful information for accurately qualifying and quantifying the impact of the long-range transported pollutants from the Asian continent in spring.

4.3.2 Enhanced mass concentrations of citric acid and their sources during the pollen episodes

Jung and Kawamura (2011) reported the elevated mass concentrations of atmospheric citric acid (range: 20–320 ng m^{-3}) in the TSP samples during the pollen episodes. They suggested that citric acid that may be directly emitted from tangerine fruit was likely adsorbed on pollens emitted from Japanese cedar trees planted around tangerine farms and then transported to the Gosan site. In order to track the source and transport mechanism of citric acid, $\delta^{13}C_{TC}$ values during the pollen episodes were plotted as a function of the fraction of citric acid carbon (citric acid-C) in TC mass (Fig. 9). It was clearly observed that the $\delta^{13}C_{TC}$ decreased as citric acid-C/TC mass ratios increase. Since the airborne pollens showed much lower $\delta^{13}C_{TC}$ values than the LTP particles in Tables 2–3, the decrease of $\delta^{13}C_{TC}$ with an increase of citric acid-C/TC ratio demonstrates an increased contribution of airborne pollen to aerosol TC. These results indicated the positive correlation between citric acid and airborne pollen concentration, suggesting that citric acid emitted from tangerine fruit might be adsorbed on airborne pollens and then transported to the Gosan site. Divergence of the $\delta^{13}C_{TC}$ values at a certain level of the citric acid-C/TC ratios shown in Fig. 9 may be explained by different adsorption efficiency of citric acid on pollens and different emission strength of citric acid from tangerine fruit.

ACPD
11, 13867–13910, 2011

The $\delta^{13}C$ values of oxalic and citric acids in the selected samples during the pollen episodes, authentic standard pollens, and tangerine fruit are shown in Table 3. The $\delta^{13}C$ of citric acid (−27.4 ‰) in the tangerine peel was similar to the $\delta^{13}C_{TC}$ in the tangerine peel (−28.1 ‰) and the Pollen_Gosan (−28.0 ‰). However, the $\delta^{13}C$ of citric acid in the Pollen_Gosan (−26.3 ‰) and KOS751 samples (−25.8 ‰) were slightly higher than that in the tangerine peel. These differences can be explained by the kinetic isotope effect (KIE, i.e., ratios of reaction rate constants for ^{12}C and ^{13}C, commonly expressed as k_{12}/k_{13}) to the isotopic fractionation in the atmospheric reactions during the atmospheric transport and aerosol sampling. Laboratory experiments as well as ambient measurements have found that aliphatic/aromatic hydrocarbons become more enriched in ^{13}C after the photochemical reactions with OH radicals (Anderson et al., 2004; Rudolph et al., 2003; Irei et al., 2006). Wang and Kawamura (2006) reported that the evaporation related isotopic fractionations and isotope exchange between organic and inorganic carbon species in diacids are insignificant at ambient temperature and pressure (thermodynamic parameters). Thus, it was suggested that citric acid in the Pollen_Gosan and KOS751 samples were originated from the tangerine peel (tangerine fruit) and then transported to the Gosan site after adsorbing to the pollens from Japanese cedar trees planted around tangerine farms.

The elevated $\delta^{13}C$ values of C_2 acid were obtained for the authentic standard pollen samples; −5.0 ‰ for the Pollen_cedar and 1.0 ‰ for the Pollen_cypress. These high $\delta^{13}C$ values of C_2 acid can be explained by the adsorption of aged C_2 acid on pollens before blowing. The $\delta^{13}C$ value of C_2 acid in the Pollen_Gosan was higher than those in the tangerine peel and the KOS751 sample. Jung and Kawamura (2011) reported similar amounts of C_2 and citric acids in the tangerine peel, suggesting that not only aged C_2 acid but directly emitted C_2 acid from the tangerine peel may be adsorbed on the Pollen_Gosan and transported together.

ACPD
11, 13867–13910, 2011

4.4 Thermal characteristics of carbonaceous particles

4.4.1 Thermal evolution pattern of OC during the carbon episodes

Thermograms of OC and EC analysis for the carbon episode samples are shown in Fig. 10 and the results are summarized in Table 4. Unique evolution patterns of OC1 and OC2 were obtained depending on the types of the carbon episodes. However, OC3 and OC4 showed similar evolution patterns among the carbon episodes as shown in Table 4; OC3 fractions in total OC = avg. 14 % to 20 % and OC4 fractions = avg. 10 % to 19 %. Similar temperature dependent EC evolution was obtained during the carbon episodes. Around 93 % of EC evolved under oven temperature < 700 °C; 39 % in EC1, 36 % in EC2, and 19 % in EC3 temperature steps. Even though sharp increase of the OC4 peak was not observed in Fig. 10 for all samples, the OC4 fractions were similar to the OC3 fractions as seen in Table 4. This discrepancy was attributed to the broad evolution of OC in the OC4 temperature step as shown in Fig. 10.

It was clearly observed that generally higher amount of OC evolved in the OC1 temperature step (24 ± 2 % in total OC) than the OC2 temperature step (9 ± 1 %) during the LTP_EC periods while more OC evolved in the OC2 temperature step (29 ± 6 %) for the samples collected during the pollen episodes. However, similar amounts of OC1 (16 ± 2 %) and OC2 (21 ± 2 %) were obtained in the LTP_NEC samples. Interestingly, OC2 (21 %) was much higher than OC1 (8 %) during the strong AD episode (KOS603) while similar amount of OC1 (19 %) and OC2 (18 %) were obtained during the weaker AD episode (KOS627).

Scatter plot between OC1 and OC2 mass concentrations are shown in Fig. 11. The regression slope of OC1 and OC2 mass concentrations in the aerosol samples collected during the pollen episodes (avg. OC2/OC1 mass ratio = 1.9 ± 0.6) was clearly distinguished from that during the LTP_EC episodes (avg. OC2/OC1 mass ratio = 0.4 ± 0.1). The less pyrolized organic carbon (PC) was obtained during the pollen episodes than those during the LTP_EC episodes. These results imply that the

ACPD
11, 13867–13910, 2011

pollen-enriched organic aerosols were less volatile and formed less PC than organic aerosols transported from East China.

Miyazaki et al. (2007) reported that medium molecular weight (>200 g mol^{-1}) water-insoluble organic species such as nonacosan, docosanol, and hexadecanoic acid evolved mostly in the OC2 temperature step, with small fractions evolving in the OC3 temperature step. Sucrose has been identified as the major water-soluble organic compound in 15 pollen species tested by Hoekstra et al. (1992). 91 % of OC in sucrose compound was evolved at the OC2 temperature step (Miyazaki et al., 2007). Thus, it was suggested that major fractions of the pollens collected at the Gosan site may have medium molecular level organic compounds.

Regression slope of OC1 versus OC2 mass concentrations showed different values between the LTP_EC and LTP_NEC episodes (Fig. 11). Much higher OC2/OC1 mass ratios (1.3 ± 0.3) were obtained during the LTP_EC episodes than the LTP_NEC episodes (0.4 ± 0.1), indicating that evolution patterns of OC1 and OC2 are quite different depending on the source regions of carbon particles and their organic chemical composition. Interestingly, higher PC fractions were obtained during the LTP_EC episodes with an average of 40 ± 4 % than the LTP_NEC episodes (24 ± 15 %). These results imply that organic aerosols transported from East China were more volatile and formed more PC than those from Northeast China.

Since air masses during the weaker AD episode were originated from Nei Mongol desert and across the northeastern part of China (Fig. 4), the thermal evolution pattern of OC during the weaker AD episode was quite similar to that during the LTP_NEC episodes as seen in Figs. 10, 11. However, even though similar air mass transport pattern was observed during the strong AD episode, the thermal evolution pattern of OC obtained for the strong AD episode was quite different from those for the LTP_NEC and weaker AD episodes. The OC2/OC1 mass ratio (2.7) obtained for the strong AD episode showed much higher value than those for the LTP_NEC (1.3 ± 0.3) and weaker AD episodes (1.0). Additionally, more PC was formed in the sample for the strong AD episode (43 %) than those for the LTP_NEC (24 ± 15 %) and weaker AD episodes (30 %).

ACPD
11, 13867–13910, 2011

Miyazaki et al. (2007) reported that lower molecular weight (<~180 g mol^{-1}) water-soluble organic compounds evolved mostly at the OC1 temperature step while the higher oven temperature was needed for the higher molecular weight of organic aerosol, resulting in an increased OC2 and OC3 fractions. Lim et al. (2010) suggested that organic acids are dominantly formed in cloud processing, whereas large multifunctional humic-like substances are dominantly formed in wet aerosols via radical-radical reactions. The increase of OC2 fraction was clearly observed for the samples of the strong AD episode than that for the weaker AD episode, suggesting that dust particles may contribute to the formation of secondary organic aerosol during the long-range atmospheric transport. As we already discussed in Sect. 3, much larger size particles were observed during the LTP_NEC episodes than the LTP_EC episodes. Higher fraction of OC2 for the LTP_NEC episodes relative to the LTP_EC episodes suggests that large size inorganic aerosols such as crustal compositions may play a certain role on the formation of secondary organic aerosols during the long-range atmospheric transport. Different sources of organic aerosols between East China and Northeast China may also contribute to the different thermal evolution patterns of OC.

4.4.2 Thermally resolved OC component versus stable carbon isotopic composition

In order to investigate the dependence of $\delta^{13}C_{TC}$ on thermally evolved OC fractions, the fractions of OC evolved at each temperature step in total OC during the pollen episodes are plotted as a function of $\delta^{13}C_{TC}$ in Fig. 12. The OC1 and OC2 fractions showed good correlations with $\delta^{13}C_{TC}$ with R^2 of 0.81 and 0.73, respectively, during the pollen episodes (Fig. 12) while almost no correlations were observed for the OC3 and OC4 fractions (data are not shown as a figure). The OC3 fractions were almost invariant regardless of $\delta^{13}C_{TC}$. Since the Pollen_Gosan had low $\delta^{13}C_{TC}$ of −28.0 ‰ (Table 3), negative correlation between the OC2 fraction and $\delta^{13}C_{TC}$ indicates that high fraction of the pollens evolved at the OC2 temperature step (300–450 °C). The positive

ACPD
11, 13867–13910, 2011

correlation between the OC1 fraction and $\delta^{13}C_{\_TC}$ indicated that more carbons evolved at the OC1 temperature step (< 300 °C) as the fraction of pollen carbon decreases.

The relationships between the OC fractions and $\delta^{13}C_{TC}$ during the LTP and AD episodes are also examined. On the contrary to the pollen episodes, almost no correlations were obtained between the OC fractions and $\delta^{13}C_{TC}$ except the OC1 fraction that gave moderate correlation of $R^2 = 0.59$ (data are not shown as a figure). The moderate correlation between the OC1 fraction and $\delta^{13}C_{TC}$ was attributed to the elevated $\delta^{13}C_{TC}$ during the strong AD episode (KOS603). Thus, if we exclude the $\delta^{13}C_{TC}$ in the KOS603 samples, no correlation was obtained between the OC1 fraction and $\delta^{13}C_{TC}$.

5 Summary and conclusion

Satellite remote sensing, air mass backward trajectories, and particulate chemical and stable carbon isotopic composition analyses allowed us to categorize the carbon episodes observed at the Gosan background super-site (33.17° N, 126.10° E) in East Asia during spring of 2007 and 2008 as long-range transported anthropogenic pollutant (LTP) from Asian continent, Asian dust (AD) accompanying with LTP, and local pollen episodes. The carbon episodes caused by the pollen episodes were characterized by the lowest $\delta^{13}C$ of TC ($\delta^{13}C_{TC}$) (avg. -25.2 ± 0.9 ‰), followed by the LTP episodes (avg. -23.3 ± 0.3 ‰) and the AD episodes (avg. -21.8 ± 2.0 ‰). Using the HCl fume treatment on the dust-enriched samples, we found that ~ 8 % in total carbon (TC) during the strong AD episode (KOS603 sample) was attributed to carbonate carbon which was not removed via the reaction with the acidic gases such as nitrogen dioxide, nitric acid, and sulfur dioxide during the long-range atmospheric transport, resulting in higher $\delta^{13}C_{TC}$.

The carbon episodes caused by the LTP were further categorized based on air mass backward trajectories, aerosol optical property, and thermal evolution pattern of organics. Ångström exponent during the LTP_EC (LTP originated from East China) episodes

ACPD
11, 13867–13910, 2011

showed higher values (1.28 to 1.40) than those (0.65 to 0.86) during the LTP_NEC (LTP from Northeast China) episodes, indicating that aerosol particles transported from East China had smaller size than those from Northeastern China. It was found that organic aerosols transported from East China were more volatile and formed more pyrolized organic carbon than those from Northeast China. Different thermal evolution pattern of organics between the LTP_NEC and LTP_EC episodes suggests different formation pathway of secondary organic aerosols during the long-range atmospheric transport. Different sources of organic aerosols between East China and Northeast China may also contribute to the different thermal evolution patterns of OC.

Based on the carbon isotope mass balance equation and the TN and TC regression approach, we found that during the pollen episodes ~40–45 % of TC was attributed to airborne pollens emitted from Japanese cedar trees planted around tangerine farms in Jeju Island. The negative correlation between the citric acid-carbon/TC ratios and $\delta^{13}C_{TC}$ and similar $\delta^{13}C$ values of citric acid between the airborne pollens (−26.3 ‰) collected at the Gosan site and tangerine fruit (−27.4 ‰) imply that citric acid emitted from tangerine fruit may be adsorbed on the airborne pollens and then transported to the Gosan site.

Acknowledgement. This work was supported by a Grant-in-Aid No. 2100923509 from the Japan Society for the Promotion of Science (JSPS) and the Environment Research and Technology Development Fund (B-0903) of the Ministry of the Environment, Japan. We appreciate the financial support of a JSPS Fellowship to J. S. Jung. We acknowledge to M. H. Lee for collecting samples at Gosan site. The authors thank NOAA Air Resources Laboratory (ARL) for the provision of the HYSPLIT transport and dispersion model and/or READY website (http://www.arl.noaa.gov/ready.php) used in this publication. We thank to Y. J. Kim and S. C. Yoon for their effort in establishing and maintaining the Gwangju and Gosan AERONET sites, respectively.

ACPD
11, 13867–13910, 2011

References

Aggarwal, S. G. and Kawamura, K.: Molecular distributions and stable carbon isotopic compositions of dicarboxylic acids and related compounds in aerosols from Sapporo, Japan: implications for photochemical aging during long-range atmospheric transport, J. Geophys. Res., 113, D14301, doi:10.1029/2007JD009365, 2008.

Anderson, R. S., Iannone, R., Thompson, A. E., Rudolph, J., and Huang L.: Carbon kinetic isotope effects in the gas-phase reactions of aromatic hydrocarbons with the OH radical at 296 ± 4 K, Geophys. Res. Lett., 31, L15108, doi:10.1029/2004GL020089, 2004.

Baltensperger, U., Dommen, J., Alfarra, R., Duplissy, J., Gaeggeler, K., Metzer, A., Facchini, M. C., Decesari, S., Finessi, E., Reinnig, C., Schott, M., Warnke, J., Hoffmann, T., Klatzer, B., Puxbaum, H., Geiser, M., Savi, M., Lang, D., Kalbere, M., and Geiser, T.: Combined determination of the chemical composition and of health effects of secondary organic aerosols: the POYSOA project, J. Aerosol Med. Pulm. Drug Delivery, 21(1), 145–154, 2008.

Birch, M. E. and Cary, R. A.: Elemental carbon-based method for monitoring occupational exposures to particulate diesel exhaust, Aerosol Sci. Technol., 25, 221–241, 1996.

Cachier, H., Buat-Ménard, M. P., Fontugne, M., and Chesselet, R.: Long-range transport of continentally-derived particulate carbon in the marine atmosphere: evidence from stable carbon isotope studies, Tellus B, 38, 161–177, 1986.

Doskey, P. V. and Ugoagwu, B. J.: Atmospheric deposition of macronutrients by pollen at a semi-remote site in northern StateWisconsin, Atmos. Environ., 23, 2761–2766, 1989.

Draxler, R. R. and Rolph, G. D.: HYSPLIT (HYbrid Single-Particle Lagrangian Integrated Trajectory) Model access via NOAA ARL READY Website (http://www.arl.noaa.gov/HYSPLIT.php), NOAA Air Resources Laboratory, Silver Spring, MD, 2011.

Dubovik, O. and King, M. D.: A flexible inversion algorithm for retrieval of aerosol optical properties from Sun and sky radiance measurements, J. Geophys. Res., 105, 20673–20696, 2000.

Forster, P., Ramaswamy, V., Artaxo, P., Berntsen, T., R. Betts, Fahey, D. W., Haywood, J., Lean, J., Lowe, D. C., Myhre, G., Nganga, J., Prinn, R., Raga, G., Schulz, M., and Van Dorland, R.: Changes in atmospheric constituents and in radiative forcing, in: Climate Change 2007: The Physical Science Basis. Contribution of Working Group I to the Fourth Assessment Report of the Intergovernmental Panel on Climate Change, edited by: Solomon, S., Qin, D., Manning, M., Chen, Z., Marquis, M., Averyt, K. B., Tignor, M., and Miller, H. L.,

ACPD
11, 13867–13910, 2011

Cambridge University Press, Cambridge, UK and New York, NY, USA, 2007.
Hoekstra, F. A., Crowe, J. H., Crowe, L. M., Van Roekel, T., and Vermeer, E.: Do phospholipids and sucrose determine membrane phase transitions in dehydrating pollen species?, Plant Cell Environ., 15, 601–606, 1992.
Huebert, B. J., Bates, T., Russell, P. B., Shi, G., Kim, Y. J., Kawamura, K., Carmichael, G., and Nakajima, T.: An overview of ACE-Asia: strategies for quantifying the relationships between Asian aerosols and their climatic impacts, J. Geophys. Res., 108(D23), 8633, doi:10.1029/2003JD003550, 2003.
IMPROVE: Spatial and Seasonal Patterns and Temporal Variability of Haze and its Constituents in the United States: Report IV, available at: http://vista.cira.colostate.edu/improve/Publications/Reports/2006/2006.htm, 2006.
Irei, S., Huang, L., Collin, F., Zhang, W., Hastie, D., and Rudolph, J.: Flow reactor studies of the stable carbon isotope composition of secondary particulate organic matter generated by OH-radical-induced reactions of toluene, Atmos. Environ., 40, 5858–5867, 2006.
Jahren, H.: The carbon stable isotope composition of pollen A, Rev. Palaeobot. Palyno., 132, 291–313, 2004.
Jung, J. and Kawamura, K.: Enhanced concentrations of citric acid in spring aerosols collected at Gosan background site in East Asia, Atmos. Environ., in revision, 2011.
Kawamura, K.: Identification of C_2–C_{10} ω-oxocarboxylic acids, pyruvic acid and C_2–C_3 α-dicarbonyls in wet precipitation and aerosol samples by capillary GC and GC-MS, Anal. Chem., 65, 3505–3511, 1993.
Kawamura, K. and Watanabe, T.: Determination of stable carbon isotopic compositions of low molecular weight dicarboxylic acids and ketocarboxylic acids in atmospheric aerosol and snow samples, Anal. Chem., 76, 5762–5768, 2004.
Kawamura, K., Kobayashi, M., Tsubonuma, N., Mochida, M., Watanabe, T., and Lee, M.: Organic and inorganic compositions of marine aerosols from East Asia: seasonal variations of water soluble dicarboxylic acids, major ions, total carbon and nitrogen, and stable C and N isotopic composition, in: Geochemical Investigation in Earth and Space Science; A Tribute to Issac R. Kaplan, The Geochemical Society, vol. 9, Elsevier, Amsterdam, 243–265, 2004.
Kim, K. W.: Physico-chemical characteristics of visibility impairment by airborne pollen in an urban area, Atmos. Environ., 41, 3565–3576, 2007.
Kundu, S., Kawamura, K., and Lee, M.: Seasonal variation of the concentrations of nitrogenous species and their nitrogen isotopic ratios in aerosols at Gosan, Jeju Island: implications for

ACPD
11, 13867–13910, 2011

atmospheric processing and source changes of aerosols, J. Geophys. Res., 115, D20305, doi:10.1029/2009JD013323, 2010.
Levy, R. C., Remer, L. A., and Dubovik, O.: Global aerosol optical properties and application 15 to Moderate Resolution Imaging Spectroradiometer aerosol retrieval over land, J. Geophys. Res., 112(D13), D13210, doi:10.1029/2006JD007815, 2007a.
Levy, R. C., Remer, L. A., Mattoo, S., Vermote, E. F., and Kaufman, Y. J.: Second-generation operational algorithm: retrieval of aerosol properties over land from inversion of moderate resolution imaging spectroradiometer spectral reflectance, J. Geophys. Res., 112(D13), D13211, doi:10.1029/2006JD007811, 2007b.
Li, J., Wang, G., Zhou, B., Cheng, C., Cao, J., Shen, Z., and An, Z.: Chemical composition and size distribution of wintertime aerosols in the atmosphere of Mt. Hua in central China, Atmos. Environ., 45, 1251–1258, 2011.
Lim, Y. B., Tan, Y., Perri, M. J., Seitzinger, S. P., and Turpin, B. J.: Aqueous chemistry and its role in secondary organic aerosol (SOA) formation, Atmos. Chem. Phys., 10, 10521–10539, doi:10.5194/acp-10-10521-2010, 2010.
Mamane, Y. and Gottlieb, J.: Heterogeneous reactions of minerals with sulfur and nitrogen oxides, J. Aerosol Sci., 20, 303–311, 1989.
Miyazaki, Y., Kondo, Y., Han, S., Koike, M., Kodama, D., Komazaki, Y., Tanimoto, H., and Matsueda, H.: Chemical characteristics of water-soluble organic carbon in the Asian outflow, J. Geophys. Res., 112, D22S30, doi:10.1029/2007JD009116, 2007.
Miyazaki, Y., Aggarwal, S. G., Singh, K., Gupta, P. K., and Kawamura, K.: Dicarboxylic acids and water-soluble organic carbon in aerosols in New Delhi, India, in winter: characteristics and formation processes, J. Geophys. Res., 114, D19206, doi:10.1029/2009JD011790, 2009.
Miyazaki, Y., Kawamura, K., and Sawano, M.: Size distributions of organic nitrogen and carbon in remote marine aerosols: Evidence of marine biological origin based on their isotopic ratios, Geophys. Res. Lett., 37, L06803, doi:10.1029/2010GL042483, 2010.
Nakajima, T., Yoon, S. C., Ramanathan, V., Shi, G. Y., Takemura, T., Higurashi, A., Takamura, T., Aoki, K., Sohn, B. J., Kim, S. W., Tsuruta, H., Sugimoto, N., Shimizu, A., Tanimoto, H., Sawa, Y., Lin, N. H., Lee, C. T., Goto, D., and Schutgens, N.: Overview of the Atmospheric Brown Cloud East Asian Regional Experiment 2005 and a study of the aerosol direct radiative forcing in East Asia, J. Geophys. Res., 112, D24S91, doi:10.1029/2007JD009009, 2007.
Narukawa, M., Kawamura, K., Li, S.-M., and Bottenheim, J. W.: Stable carbon isotopic ratios and ionic composition of the high-Arctic aerosols: an increase in d^{13}C values from winter to

ACPD
11, 13867–13910, 2011

spring, J. Geophys. Res., 113, D02312, doi:10.1029/2007JD008755, 2008.
Novakov, T. and Penner, J. E.: Large contribution of organic aerosols to cloud-condensation-nuclei concentrations, Nature, 365, 823–826, 1993.
O'Dowd, C. D., Facchini, M. C., Cavalli, F. C., Ceburnis, D., Mircea, M., Decesari, S., Fuzzi, S., Yoon, Y. J., and Putaud, J. P.: Biogenically drived organic contribution to marine aerosol, Nature, 431, 676–679, 2004.
Oh, J. W., Lee, H. B., Lee, H. R., Pyun, B. Y., Ahn, Y. M., Kim, K. E., Lee, S. Y., Lee, S. I.: Aerobiological study of pollen and mold in Seoul, Korea, Allergol. Int., 47, 263–270, 1998.
Palacios, I. S., Molina, R. T., and Rodriguez, A. F. M.: The importance of interactions between meteorological conditions when interpreting their effect on the dispersal of pollen from homogeneously distributed sources, Aerobiologia, 23, 17–26, 2007.
Porsbjerg, C., Rasmussen, A., and Backer, A.: Airborne pollen in Nuuk, Greenland, and the importance of meteorological parameters, Aerobiologia, 19, 29–37, 2003.
Puc, M. and Wolski, T.: Betula and Populus pollen counts and meteorological conditions in Szczencin, Poland, Ann. Agr. Environ. Med., 9, 65–69, 2002.
Remer, L. A., Kaufman, Y. J., Tanr, D., Mattoo, S., Chu, D. A., Martins, J. V., Li, R.-R., Ichoku, C., Levy, R. C., Kleidman, R. G., Eck, T. F., Vermonte, E., and Holben, B. N.: The MODIS aerosol algorithm, products, and validation, J. Atmos. Sci., 62, 947–973, 2005.
Rolph, G. D.: Real-time Environmental Applications and Display sYstem (READY) Website, available at: http://www.arl.noaa.gov/ready.php, NOAA Air Resources Laboratory, Silver Spring, MD, 2011.
Rousseau, D.-D., Schevin, P., Ferrier, J., Jolly, D., Andreasen, T., Ascanius, S. E., Hendriksen, S.-E., and Poulsen, U.: Long-distance pollen transport from North America to Greenland in spring, J. Geophys. Res., 113, G02013, doi:10.1029/2007JG000456, 2008.
Rudolph, J., Anderson, R. S., Czapiewski, K. V., Czuba, E., Ernst, D., Gillespie, T., Huang, L., Rigby, C., and Thompson, A. E.: The stable carbon isotope ratio of biogenic emissions of isoprene and the potential use of stable isotope ratio measurements to study photochemical processing of isoprene in the atmosphere, J. Atmos. Chem., 44, 39–55, 2003.
Solomon, W. R.: Airborne pollen: a brief life, J. Allergy Clin. Immun., 109 (6), 895–900, 2002.
Turekian, V. C., Macko, S. A., and Keene, W. C.: Concentrations, isotopic compositions, and sources of size-resolved, particulate organic carbon and oxalate in near-surface marine air at Bermuda during spring, J. Geophys. Res., 108(D5), 4157, doi:10.1029/2002JD002053, 2003.

ACPD
11, 13867–13910, 2011

Underwood, G. M., Song, C., Phandis, M., Carmichael, G., and Grassian, V.: Heterogeneous reactions of NO_2 and HNO_3 on oxides and mineral dust: a combined laboratory and modeling study, J. Geophys. Res., 106, 18,055–18,066, 2001.

Wang, H. and Kawamura, K.: Stable carbon isotopic composition of low-molecular weight dicarboxylic acids and ketoacids in remote marine aerosols, J. Geophys. Res., 111, D07304, doi:10.1029/2005JD006466, 2006.

Wang, G., Xie, M., Hu, S., Gao, S., Tachibana, E., and Kawamura, K.: Dicarboxylic acids, metals and isotopic compositions of C and N in atmospheric aerosols from inland China: implications for dust and coal burning emission and secondary aerosol formation, Atmos. Chem. Phys., 10, 6087–6096, doi:10.5194/acp-10-6087-2010, 2010.

Yang, H., Yu, J. Z., Ho, S. S. H., Xu, J., Wu, W. S., Wan, C. H., Wang, X., Wang, X., and Wang, L.: The chemical composition of inorganic and carbonaceous materials in $PM_{2.5}$ in Nanjing, China, Atmos. Environ., 39, 3735–3749, 2005.

Ye, B., Ji, X., Yang, H., Yao, X., Chan, C. K., Cadle, S. H., Chan, T., and Mulawa, P. A.: Concentration and chemical composition of $PM_{2.5}$ in Shanghai for a 1-year period, Atmos. Environ., 37, 499–510, 2003.

Zhang, Y., Sunwoo, Y., Kotamarthi, V., and Carmichael, G.: Photochemical oxidant processes in the presence of dust: An evaluation of the impact of dust on particulate nitrate and ozone formation, Am. Meteorol. Soc., 33, 813–824, 1994.

ACPD

11, 13867–13910, 2011

Table 1. Specification of sampling, PM_{10} mass concentration, non-sea-salt calcium ion (nss-Ca^{2+}), and Ångström exponent at the Gosan site during the carbon episodes in spring of 2007 and 2008.

Sample ID	Category[1]	Period	PM_{10} mass[2] ($\mu g\,m^{-3}$)	nss-Ca^{2+} ($\mu g\,m^{-3}$)	Ångström exponent[3]
KOS603	AD	30 Mar–2Apr 2007	362 (3704)	7.6	N/A
KOS606	LTP_EC	6–9 Apr 2007	70 (158)	1.6	1.40 ± 0.18
KOS608	Pollen	11–13 Apr 2007	47 (86)	1.5	1.26 ± 0.21
KOS609	Pollen	13–16 Apr 2007	50 (120)	0.8	1.03 ± 0.24
KOS610	Pollen	16–18 Apr 2007	33 (52)	0.6	N/A
KOS611	Pollen	18–20 Apr 2007	38 (54)	0.5	1.37 ± 0.37
KOS612	Pollen	20–23 Apr 2007	37 (80)	0.5	N/A
KOS613	Pollen	23–25 Apr 2007	61 (94)	1.3	0.57 ± 0.06
KOS614	LTP_EC	25–27 Apr 2007	129 (180)	5.5	1.28 ± 0.15
KOS619	LTP_EC	7–9 May 2007	94 (168)	2.7	1.40 ± 0.07
KOS621	LTP_NEC	11–14 May 2007	74 (126)	3.1	0.86 ± 0.46
KOS623	LTP_NEC	17–18 May 2007	107 (148)	4.7	0.65 ± 0.13
KOS627	AD	25–28 May 2007	157 (286)	7.3	0.37 ± 0.06
KOS751	Pollen	16–21 Apr 2008	59 (184)	0.4	1.18 ± 0.08
KOS752	Pollen	21–24 Apr 2008	53 (82)	0.4	N/A

[1] AD: Asian dust episode, Pollen: pollen episode, LTP_EC: long-range transported pollution episode originated from East China, LTP_NEC: long-range transported pollution episode originated from Northeast China.

[2] Average (maximum).

[3] Ångström exponents during the KOS606, 608, and 751 sampling periods were obtained from the Gwangju AERONET site which is located at ~200 km north of the Gosan site.

ACPD
11, 13867–13910, 2011

Table 2. Concentrations of organic (OC) and elemental carbons (EC), total carbon (TC), total nitrogen (TN), and stable carbon isotopic composition ($\delta^{13}C$) in the total suspended particle (TSP) samples collected at the Gosan site during the carbon episodes.

Parameters	Category	Min.	Max.	Avg.	S.D.
$\delta^{13}C$ (‰)	AD	−23.3	−20.4	−21.8	2.0
	LTP	−23.5	−23.0	−23.3	0.3
	Pollen	−26.2	−23.5	−25.2	0.9
TC ($\mu g\,C\,m^{-3}$)	AD	12	19	16	4.6
	LTP	11	24	15	6.0
	Pollen	7.5	28	16	6.7
OC ($\mu g\,C\,m^{-3}$)	AD	9.3	16	13	4.5
	LTP	6.9	19	12	4.7
	Pollen	6.9	27	14	8.2
EC ($\mu g\,C\,m^{-3}$)	AD	3.6	4.0	3.8	0.2
	LTP	2.2	6.1	3.7	1.5
	Pollen	1.3	6.0	2.5	1.5
OC/EC ratio	AD	2.3	4.3	3.3	1.4
	LTP	2.7	3.8	3.2	0.4
	Pollen	3.8	12	5.8	2.6
TN ($\mu g\,N\,m^{-3}$)	AD	4.8	11	7.7	4.0
	LTP	4.9	25	11	8.2
	Pollen	2.3	7.0	4.8	1.5
TC/TN ratio	AD	1.2	3.9	2.5	1.9
	LTP	0.96	2.3	1.6	0.58
	Pollen	1.8	5.3	3.5	1.2

ACPD
11, 13867–13910, 2011

Table 3. Stable carbon isotopic compositions ($\delta^{13}C$) of TC and oxalic and citric acids in the selected samples during the pollen episodes, pollens, and tangerine fruit.

Samples	$\delta^{13}C$ (‰)		
	TC[4]	Oxalic acid[5]	Citric acid[5]
KOS611	−25.0	−16.6 ± 0.03	−24.7 ± 0.06
KOS751	−26.2	−21.1 ± 0.3	−25.8 ± 0.3
KOS752	−26.1	−21.0 ± 0.3	−25.9 ± 0.3
Pollen_Gosan[1]	−28.0	–	–
WS[2] Pollen_Gosan	−24.7	−16.6 ± 0.08	−26.3 ± 0.2
Pollen_cedar[3]	−25.4	–	–
WS Pollen_cedar	−26.1	−5.0 ± 0.2	–
Pollen_cypress[3]	−23.3	–	–
WS Pollen_cypress	−25.0	1.0 ± 0.03	–
WS Tangerine juice	−27.0	–	−29.3 ± 0.4
WS Tangerine peel	−28.1	−19.5 ± 0.5	−27.4 ± 0.4

[1] Pollen_Gosan represent airborne pollens separated from the KOS751 sample.
[2] WS represents water-soluble fraction of sample.
[3] Pollen_cedar and Pollen_cypress represent authentic standard pollens from Japanese cedar and Japanese cypress, respectively.
[4] The analytical error for $\delta^{13}C$ of TC measurement was 2.3 %.
[5] Average ± standard deviation.

ACPD
11, 13867–13910, 2011

Table 4. Average mass fractions of OC evolved at each temperature step in total OC and OC2/OC1 mass ratios according to the categorized carbon episodes.

Category	The mass fraction in total OC (%)					OC2/OC1
	OC1[1]	OC2[1]	OC3[1]	OC4[1]	PC[2]	mass ratio
Pollen	15±3	29±6	18±2	12±6	26±7	1.9±0.6
LTP_EC	24±2	9±1	14±1	13±1	40±4	0.4±0.1
LTP_NEC	16±2	21±2	20±7	19±7	24±15	1.3±0.3
AD(KOS603)	8	21	18	10	43	2.7
AD(KOS627)	19	18	16	16	30	1.0

[1] OC1, OC2, OC3, and OC4 represent the carbon evolved at a temperature of 300 °C, 450 °C, 600 °C, and 650 °C, respectively.
[2] PC represents the pyrolized organic carbon during the OC analysis mode in an inert atmosphere (pure helium).

ACPD
11, 13867–13910, 2011

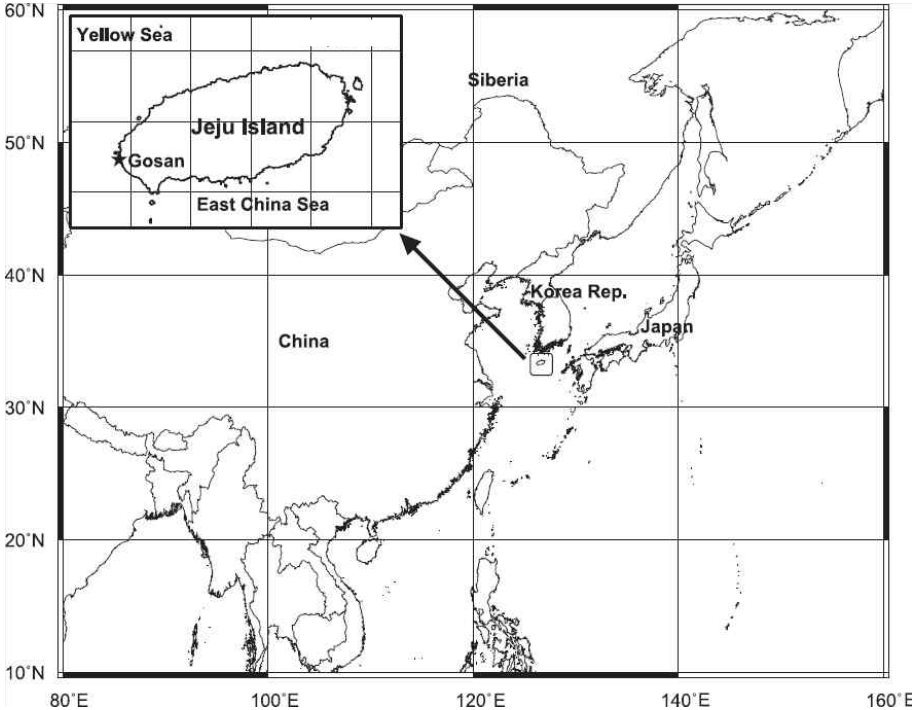

Fig. 1. Image map of Gosan supersite (33.17° N, 126.10° E) in Jeju Island, located approximately 100 km south of the Korean peninsula.

ACPD
11, 13867–13910, 2011

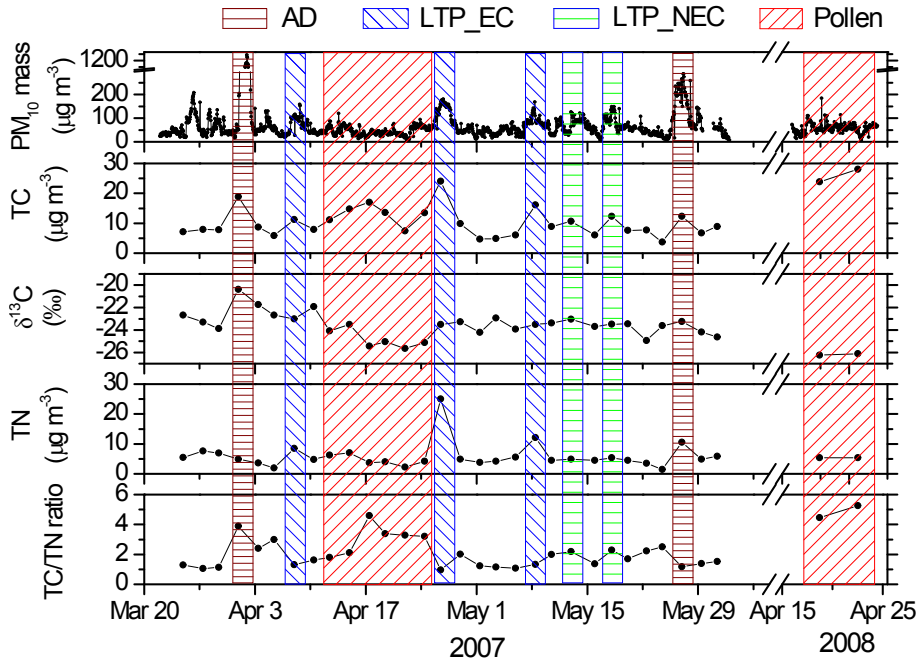

Fig. 2. Temporal variations of mass concentrations of PM_{10}, total carbon (TC), and total nitrogen (TN), stable carbon isotopic compositions of TC ($\delta^{13}C_{TC}$), and TC/TN ratios at the Gosan site during 23 March to 1 June of 2007 and 16–24 April of 2008. AD and Pollen represent Asian dust and airborne pollen episodes, respectively. LTP_EC and LTP_NEC represent the long-range transported pollutants originated from East China and Northeast China, respectively.

ACPD
11, 13867–13910, 2011

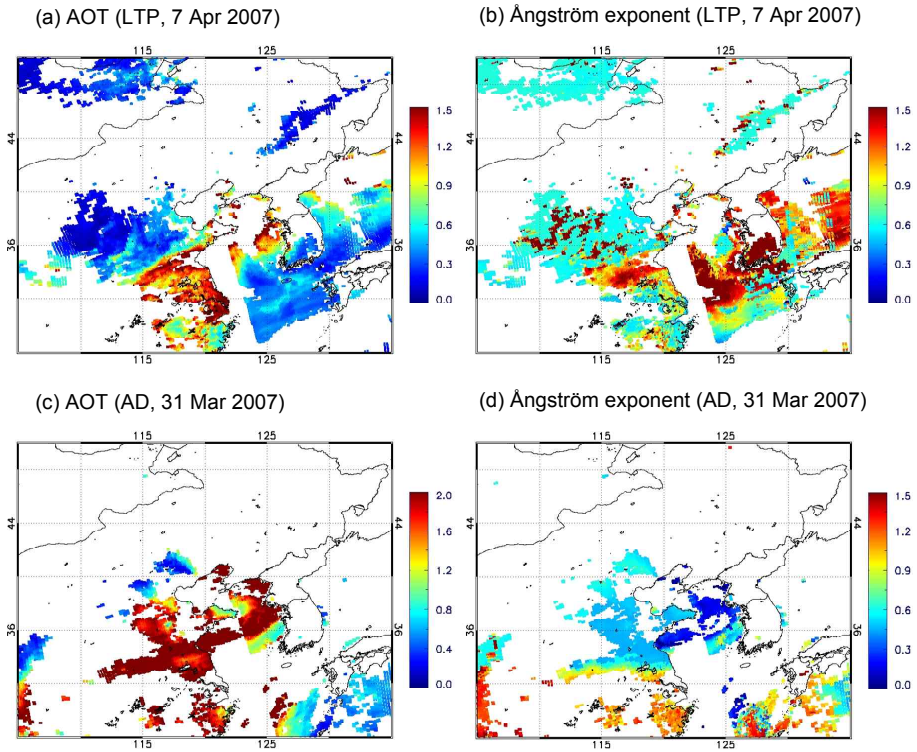

Fig. 3. **(a)** MODIS aerosol optical thickness (AOT) and **(b)** Ångström exponent during the selected day (7 April 2007) of the LTP episodes. Those during the selected day (31 March 2007) of the AD episodes are shown in **(c, d)**.

ACPD
11, 13867–13910, 2011

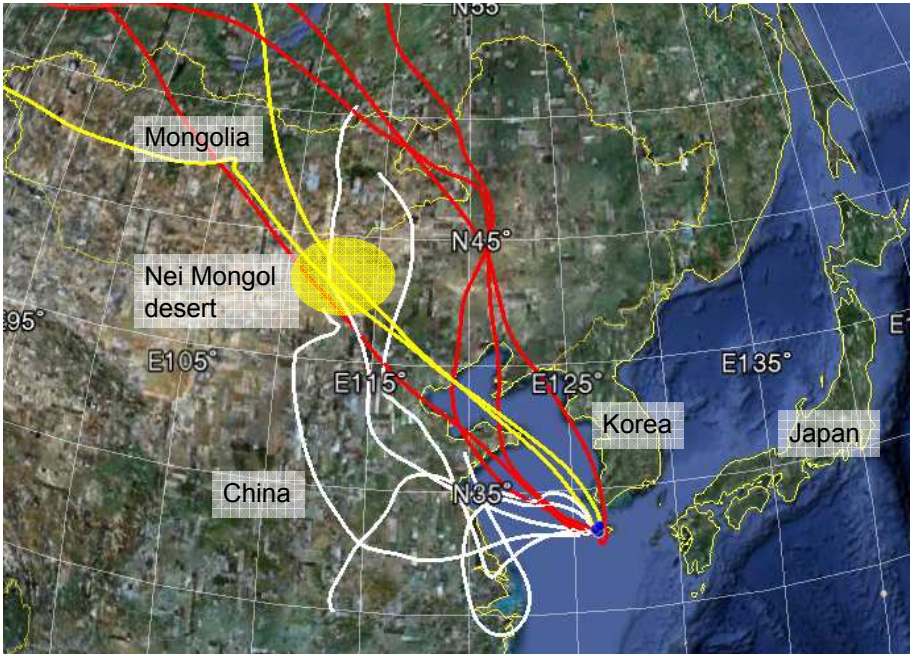

Fig. 4. HYSPLIT air mass backward trajectories arriving at the Gosan site. White, red, and yellow represent air mass trajectories during the LTP_EC, LTP_NEC, and AD episodes, respectively.

ACPD
11, 13867–13910, 2011

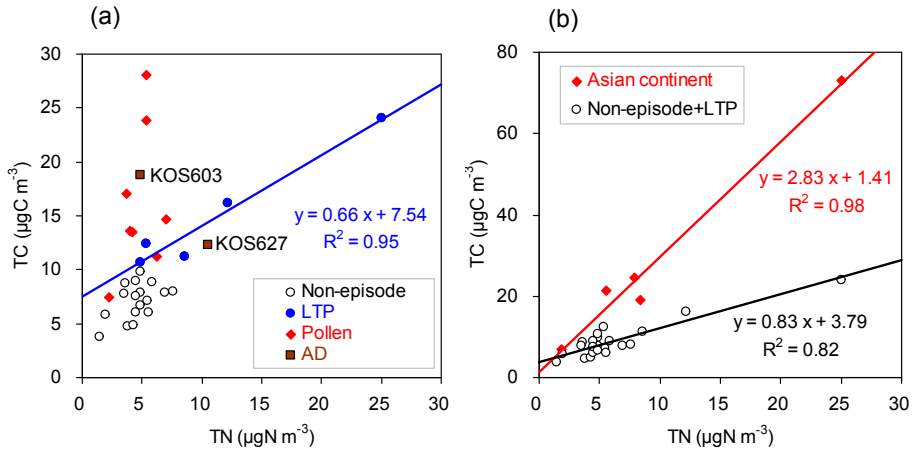

Fig. 5. **(a)** Scatter plot between mass concentrations of TN versus TC during the entire sampling period. Filled blue circle, red diamond, and brown rectangular represent the LTP, Pollen, and AD episodes, respectively. **(b)** Mass concentrations of TN and TC during the non-episode plus LTP episode are compared to those from previous studies in the Asian continent. TN and TC values in the Asian continent were obtained from the urban cities of China: Shanghai ($PM_{2.5}$, winter and spring) (Ye et al., 2003), Nanjing ($PM_{2.5}$, winter) (Yang et al., 2005), Baoji (PM_{10}, spring) (Wang et al., 2010) as well as the Hua mountain site (PM_{10}, winter) (Li et al., 2011). The analytical errors for TC and TN mass concentrations at the Gosan site were 2.3 % and 5.2 %, respectively.

ACPD
11, 13867–13910, 2011

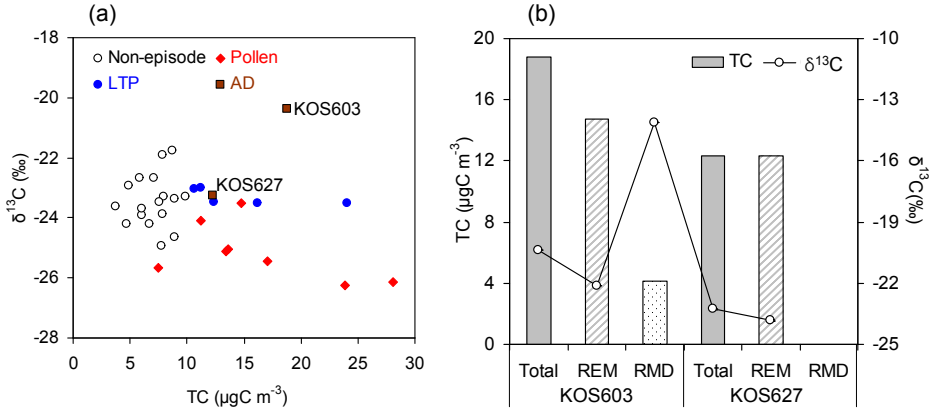

Fig. 6. **(a)** $\delta^{13}C_{TC}$ values as a function of TC mass concentrations and **(b)** TC mass concentrations and $\delta^{13}C_{TC}$ values in the aerosol samples collected during the AD episodes before and after the HCl fume treatment. REM and RMD represent the remained carbon and the removed carbon after the HCl fume treatment, respectively. KOS603 and KOS627 samples were collected during the strong AD (30 Mar–2 Apr 2007) and weaker AD episodes (25–28 May 2007), respectively. The standard deviation of $\delta^{13}C_{TC}$ was ~0.03‰ and its analytical error was ~0.1 %.

ACPD
11, 13867–13910, 2011

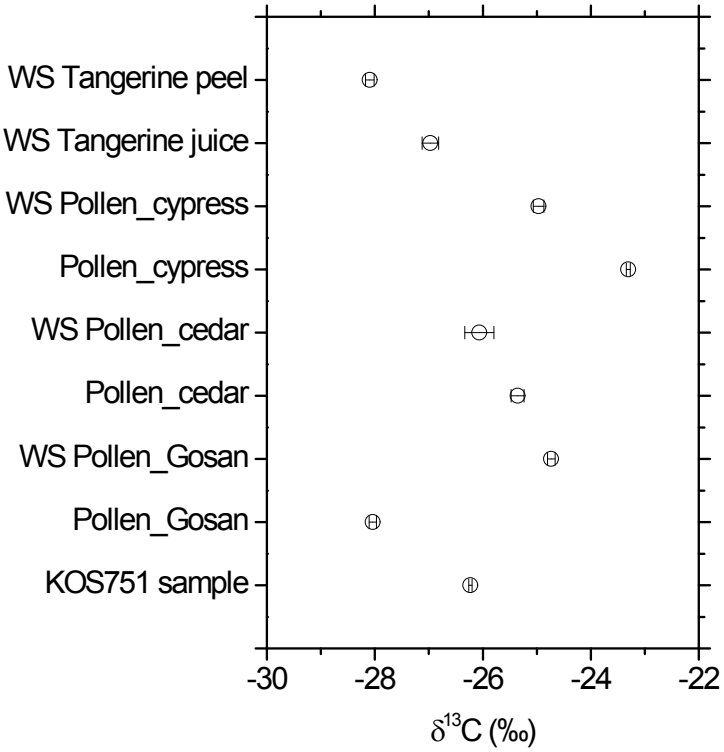

Fig. 7. $\delta^{13}C_{TC}$ values in the airborne pollens collected at the Gosan site (Pollen_Gosan), authentic standard pollens from Japanese cedar and Japanese cypress, tangerine fruit, and the filter sample collected during the severe pollen episode (KOS751). WS represents water-soluble fraction of the samples. The error bar represents the standard deviation of the duplicate analyses of the sample.

ACPD
11, 13867–13910, 2011

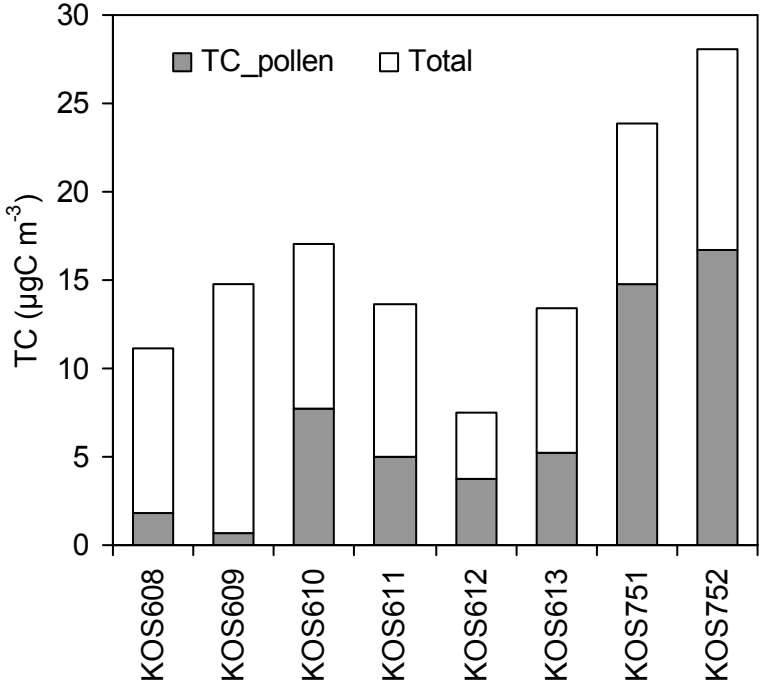

Fig. 8. Temporal variations of mass concentrations of TC and airborne pollen carbon (TC_pollen) determined using the isotope mass balance equation.

ACPD
11, 13867–13910, 2011

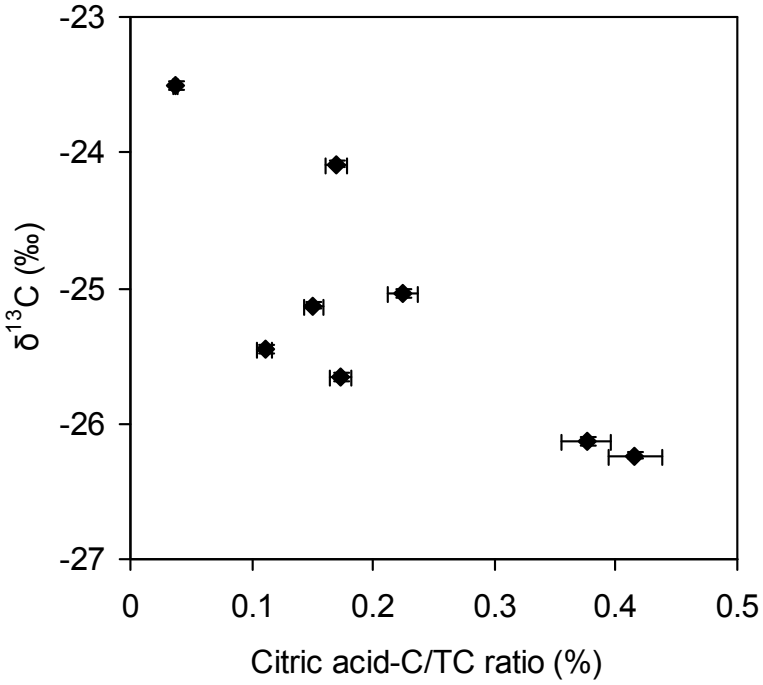

Fig. 9. $\delta^{13}C_{TC}$ values as a function of citric acid carbon (citric acid-C) to TC mass ratios during the pollen episodes.

ACPD
11, 13867–13910, 2011

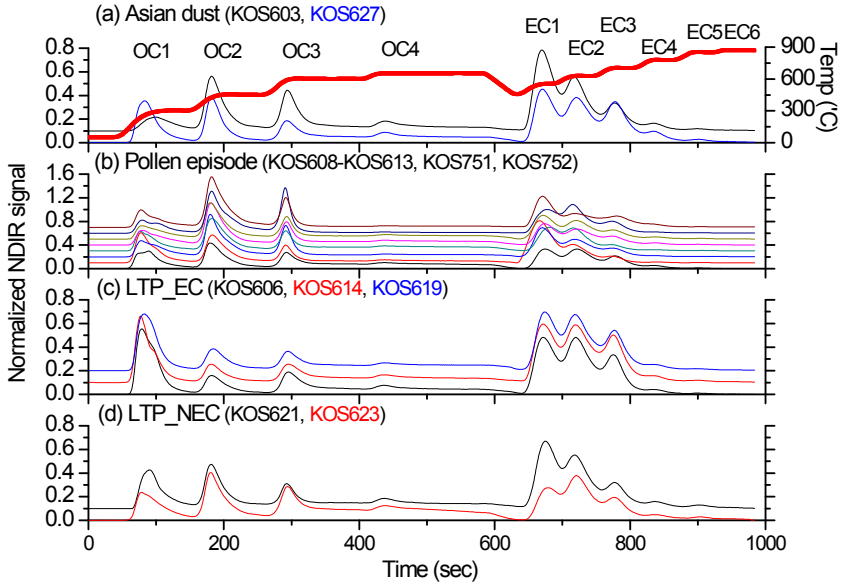

Fig. 10. Thermograms of carbonaceous particles during the **(a)** AD, **(b)** pollen, **(c)** LTP_EC, and **(d)** LTP_NEC episodes. The analytical errors of OC and EC measurements were 5 % and 3 %, respectively.

ACPD
11, 13867–13910, 2011

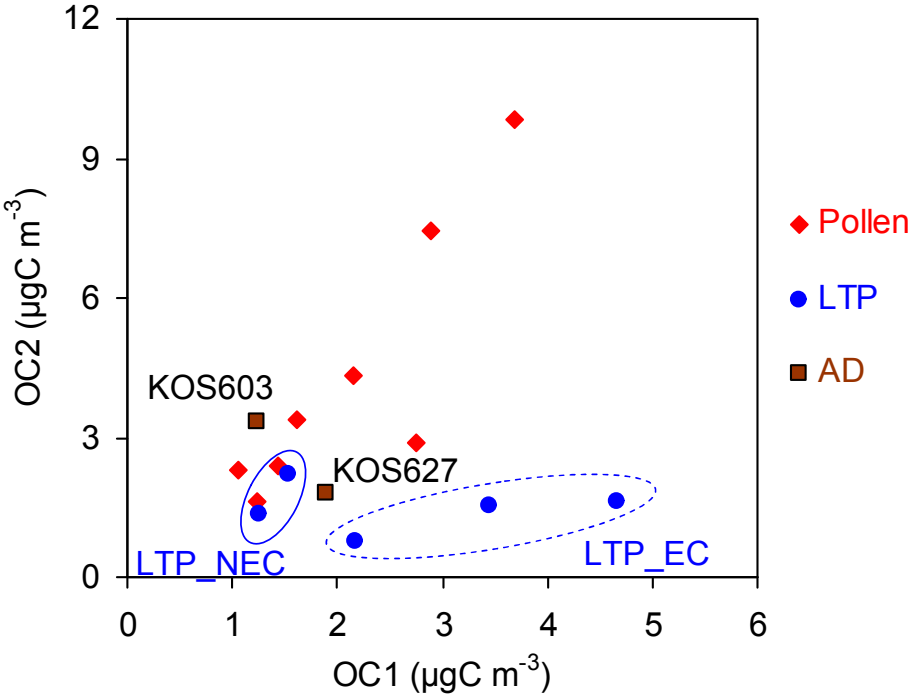

Fig. 11. Scatter plot of mass concentrations of OC1 vs. OC2. The pollen, LTP, and AD episodes are shown as filled red diamond, blue circle, and brown rectangular, respectively. OC1 and OC2 represent organic carbons evolved at 300 °C and 450 °C, respectively.

ACPD
11, 13867–13910, 2011

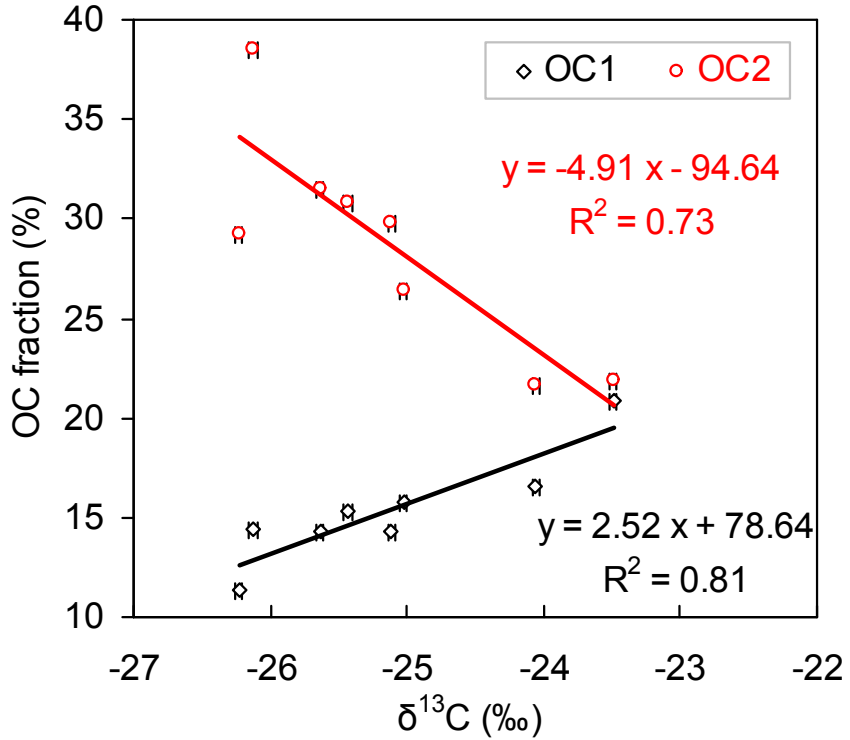

Fig. 12. Scatter plot of $\delta^{13}C_{TC}$ versus OC1 and OC2 fractions in total OC during the pollen episodes. The error bar in x-axis represents the analytical error of $\delta^{13}C_{TC}$ measurement.

ACPD
11, 13867–13910, 2011